学位論文

Postnatal development of subfields in the core region of the mouse auditory cortex
（マウス聴覚野のコア領域における生後のサブフィールドの発達）

譚 非凡

熊本大学大学院医学教育部博士課程医学専攻 HIGO Program 4 years コース

指導教員

宋 文杰　教授

熊本大学大学院医学教育部博士課程医学専攻知覚生理学

2021年3月

学　位　論　文

Title of Thesis : **Postnatal development of subfields in the core region of the mouse auditory cortex**
（マウス聴覚野のコア領域における生後のサブフィールドの発達）

Name of Author : Chen Feifan

Name of supervisor : Professor Wen-Jie Song
Department of Sensory and Cognitive Physiology, Medical Sciences Major, Doctoral Course of the Graduate School of Medical Sciences

Name of examiner : Professor Takaichi Fukuda Department of Anatomy and Neurobiology

Professor Kenji Shimamura Department of Brain Morphogenesis

Professor Kazuya Iwamoto Department of Molecular Brain Science

Professor Hidenobu Mizuno Department of IRCMS

March 2021

Hearing Research 400 (2021) 108138

Contents lists available at ScienceDirect

Hearing Research

journal homepage: www.elsevier.com/locate/heares

Research Paper

Postnatal development of subfields in the core region of the mouse auditory cortex

Feifan Chen[a,b], Makoto Takemoto[a], Masataka Nishimura[a], Ryohei Tomioka[a], Wen-Jie Song[a,b,c,*]

[a] Department of Sensory and Cognitive Physiology, Graduate School of Medical Sciences, Kumamoto University, Japan
[b] Program for Leading Graduate Schools HIGO Program, Kumamoto University, Kumamoto, Japan
[c] Center for Metabolic Regulation of Healthy Aging, Faculty of Life Sciences, Kumamoto University, Kumamoto 860-8556, Japan

ARTICLE INFO

Article history:
Received 27 September 2020
Revised 24 November 2020
Accepted 25 November 2020
Available online 29 November 2020

Keywords:
Anterior auditory field
Cortical magnification factor
Primary auditory cortex
Real-time optical imaging

ABSTRACT

The core region of the rodent auditory cortex has two subfields: the primary auditory area (A1) and the anterior auditory field (AAF). Although the postnatal development of A1 has been studied in several mammalian species, few studies have been conducted on the postnatal development of AAF. Using a voltage-sensitive-dye-based imaging method, we examined and compared the postnatal development of AAF and A1 in mice from postnatal day 11 (P11) to P40. We focused on the postnatal development of tonotopy, the relative position between A1 and AAF, and the properties of tone-evoked responses in the subfields. Tone-evoked responses in the mouse auditory cortex were first observed at P12, and tonotopy was found in both A1 and AAF at this age. Quantification of tonotopy using the cortical magnification factor (CMF; octave difference per unit cortical distance) revealed a rapid change from P12 to P14 in both A1 and AAF, and a stable level from P14. A similar time course of postnatal development was found for the distance between the 4 kHz site in A1 and AAF, the distance between the 16 kHz site in A1 and AAF, and the angle between the frequency axis of A1 and AAF. The maximum amplitude and rise time of tone-evoked signals in both A1 and AAF showed no significant change from P12 to P40, but the latency of the responses to both the 4 kHz and 16 kHz tones decreased during this period, with a more rapid decrease in the latency to 16 kHz tones in both subfields. The duration of responses evoked by 4 kHz tones in both A1 and AAF showed no significant postnatal change, but the duration of responses to 16 kHz tones decreased exponentially in both subfields. The cortical area activated by 4 kHz tones in AAF was always larger than that in A1 at all ages (P12-P40). Our results demonstrated that A1 and AAF developed in parallel postnatally, showing a rapid maturation of tonotopy, slow maturation of response latency and response duration, and a dorsal-to-ventral order (high-frequency site to low-frequency site) of functional maturation.

1. Introduction

It is now well established that the sensory cortices of the mammalian brain continue to develop postnatally to achieve adult patterns in terms of the accuracy of spatial representation of the sensory world, the innervation pattern of bilateral inputs, the precise pattern of axonal and dendritic arbors, and other anatomical and physiological features (Shatz, 1997; Espinosa and Stryker, 2012; Erzurumlu and Gaspar, 2012; Sakano, 2020). While many developmental studies have been carried out on the visual and somatosensory cortices (Inan and Crair, 2007; Fox, 2009; Espinosa and Stryker, 2012), only a limited number of studies have been conducted on the mammalian auditory cortex (Zhang et al., 2001; Polley et al., 2013; Sollini et al., 2018; see Kral and Pallas, 2011 for a review). The auditory cortex in primates has three regions: the core region, belt region surrounding the core, and parabelt region lateral to the belt; each region has multiple subfields (Kaas and Hackett 2000). The rodent auditory cortex has a similar organization but without an apparent parabelt region; the core region is composed of the two largest subfields, the primary area (A1) and the anterior auditory field (AAF) rostral to A1, and the belt region consists of many smaller subfields (Stiebler et al., 1997; Budinger et al., 2000; Wallace et al., 2000; Nishimura et al., 2007; Polley et al., 2007; Sawatari et al., 2011; Guo et al., 2012;

* Corresponding author at: Department of Sensory and Cognitive Physiology, Graduate School of Medical Sciences, Kumamoto University, Kumamoto 860-8556, Japan.
E-mail address: song@kumamoto-u.ac.jp (W.-J. Song).

https://doi.org/10.1016/j.heares.2020.108138
0378-5955/

Takemoto et al., 2014; Saldeitis et al., 2014; Romero et al., 2020; Nakata et al., 2020; reviewed in Tsukano et al., 2017). Both A1 and AAF in mice have a clear spatial representation of tone frequency, or tonotopy (Stiebler et al., 1997; Hackett et al., 2011; Sawatari et al., 2011; Guo et al., 2012; Takemoto et al., 2014; Shepard et al. 2015; Tsukano et al., 2015; Blundon et al., 2017; Nakata et al., 2020). Functionally, AAF appears to be more involved in temporal processing, whereas A1 may favor spectral processing (Hackett et al., 2011; Guo et al., 2012; Polley et al., 2007; Linden et al., 2003; Sołyga and Barkat, 2019). It is also known that A1 streams auditory information for audio-visual association at the cortical and subcortical levels, while AAF sends auditory output for association with somatomotor information in the cortex (Nakata et al., 2020).

One central issue in the postnatal development of the auditory cortex is to ascertain when cortical neurons start to respond to sound stimulation. This issue has been addressed in both mice (Polley et al., 2013) and rats (Geal-Dor et al., 1993; de Villers-Sidani et al., 2007). A1 neurons start to respond to tone stimulation from postnatal day 11 (P11) in both animals, with a rapid decrease in the threshold for eliciting a response after that. Another issue is the development of tonotopy. It has been shown in rat A1 that adult-like tonotopy is observed from P14 (de Villers-Sidani et al., 2007). Postnatal changes in the size of rat A1 have also been reported to increase monotonically from P11, reaching an adult level at P14 (de Villers-Sidani et al., 2007), although the overall area of the auditory cortex has been reported to show a transient peak at P16 (Zhang et al., 2001; Chang and Merzenich, 2003). Postnatal development of frequency tuning and spatial tuning has also been studies in A1 of mice and ferrets (Mrsic-Flogel et al., 2003, 2006; Polley et al., 2013).

The postnatal development of AAF, however, has seldomly been the subject of study (Babola et al., 2018). How the relative position between A1 and AAF develops during postnatal life is also unknow. Here, we aimed to examine and compare the postnatal development of both A1 and AAF in mice, using a real-time high-resolution optical imaging technique, to address the following specific questions: 1) when the two subfields start to exhibit tonotopy and how tonotopy develops during postnatal development, 2) how the size of each subfield and the relative position between the two subfields change with postnatal development, and 3) how the properties of tone-evoked responses change in the subfields with postnatal development. We made recordings from P11 but observed tone-evoked responses from P12 when both A1 and AAF showed clear tonotopy. The quantitation of tonotopy using the cortical magnification factor (CMF), the frequency difference represented per unit of cortical distance, revealed a rapid decrease to a stable level at P14. The relative position between A1 and AAF developed in a similar time course. However, the response latency in the subfields showed a much slower development. These results demonstrate that A1 and AAF developed in parallel during the first postnatal month.

2. Material and methods

2.1. Animals

ICR mice aged from P11 to P40, purchased from Japan SLC (Hamamatsu, Japan), were used for the experiments. All animals were maintained in a breeding room of our facility with a 12 h light/dark cycle and food and water available *ad libitum*. All experiments were approved by the Committee for Animal Experiments of Kumamoto University and performed in accordance with the Guidelines for Use of Animals in Experiments of Kumamoto University.

2.2. Voltage-sensitive dye imaging

Voltage-sensitive dye imaging was performed as reported previously (Sawatari et al., 2011; Takemoto et al., 2014; Nakata et al., 2020; Fig. 1A), with a slight modification. In brief, the animals were anesthetised with a mixture of ketamine and xylazine (initial dose: ketamine 80 mg/kg, xylazine 8 mg/kg; supplemental doses: ketamine 40 mg/kg/h, xylazine 4 mg/kg/h). The external ear canal was open from P12, but was partially closed at P11; we opened the ear canal with forceps and kept the canal open by inserting a short plastic tubing in the canal for P11 mice. Animal's body temperature was maintained at 36.5 ± 0.5 °C with a heating blanket, and its heart rate was monitored throughout the experiment. The top of a flat head screw was attached to the skull with adhesive resin cement (Super-Bond CandB, Sun Medical, Shiga, Japan), and the screw was used to hold the animal's head with a custom-made head holder during surgery and recording. A cranial window over the left auditory cortex was made with great care, with an effort to make the dorsal edge of the window parallel to the midline. The dura mater over the cortex was removed, and the exposed cortex was subsequently stained twice for 45 min each time with the voltage-sensitive dye RH-1691 (0.6 mg/ml in saline, Optical Imaging Ltd., Israel) (Shoham et al., 1999). After staining, the cortex was washed and covered with 0.5% agarose in saline. No evident swelling of the cortex was observed from post-craniotomy to the end of experiment. As acoustic stimuli, pure tones (4, 8, or 16 kHz, 50 ms duration, 10 ms onset and offset cosine ramps, 30–80 dB SPL) were produced and delivered with TDT System 3 hardware and software (Tucker-Davis Technologies, FL, USA), calibrated with a sound level meter (Brüel and Kjær, Nærum, Denmark), and applied to the right ear of the animal in a double-walled soundproof room. The data presented were obtained using stimulations at 60 dB SPL for 4- and 16-kHz tones, and 30–60 dB SPL for 8 kHz tones. Optical signals were detected with a high-resolution complementary metal oxide semiconductor imaging system (100 × 100 pixels; MiCAM Ultima, BrainVision, Tokyo, Japan) at a sampling interval of 1 ms. The recording field was 3.15 × 3.15 mm^2, and one edge of the recording field was made quasi-parallel to the midline. Fractional fluorescence signals ($\Delta F/F_0$) were calculated and averaged for 16 consecutive recordings for each tone frequency, then encoded in color and superimposed on the cortical surface using custom-made software (Nishimura et al., 2007).

2.3. Data analyses

Optical recordings were analyzed as previously described (Nishimura and Song, 2014). The fluorescence signals were first spatially low-pass filtered (< 0.33 cycle/pixel; spatial resolution: ~95 μm in diameter). The basal fluorescence signal level (F_0) was calculated by averaging 50 frames before the stimulus onset. The cortical response was calculated as fractional changes in fluorescence ($\Delta F/F_0$) in each pixel from the spatially filtered signals to suppress the effect of spatially non-uniform staining. $\Delta F/F_0$ was then temporally low-pass filtered (< 167 Hz). The standard deviation (SD) of the first 50-frame $\Delta F/F_0$ before the stimulus onset was used to determine the response latency for each pixel, defined as the time interval from the stimulus onset to when the response exceeds three times the SD. To obtain the maximum response in A1 or AAF, the pixel with the largest peak was first detected, and recordings from the surrounding eight pixels were added and averaged (average over nine pixels). The peak of the averaged results was defined as the maximum response. The onset response to a tone in A1 and AAF was defined as the binarized response using a threshold of 20% of the subfield's maximum response at the time (frame) when the response in the pixel showing the largest peak reached 20% of the maximum response in the ascending phase. The

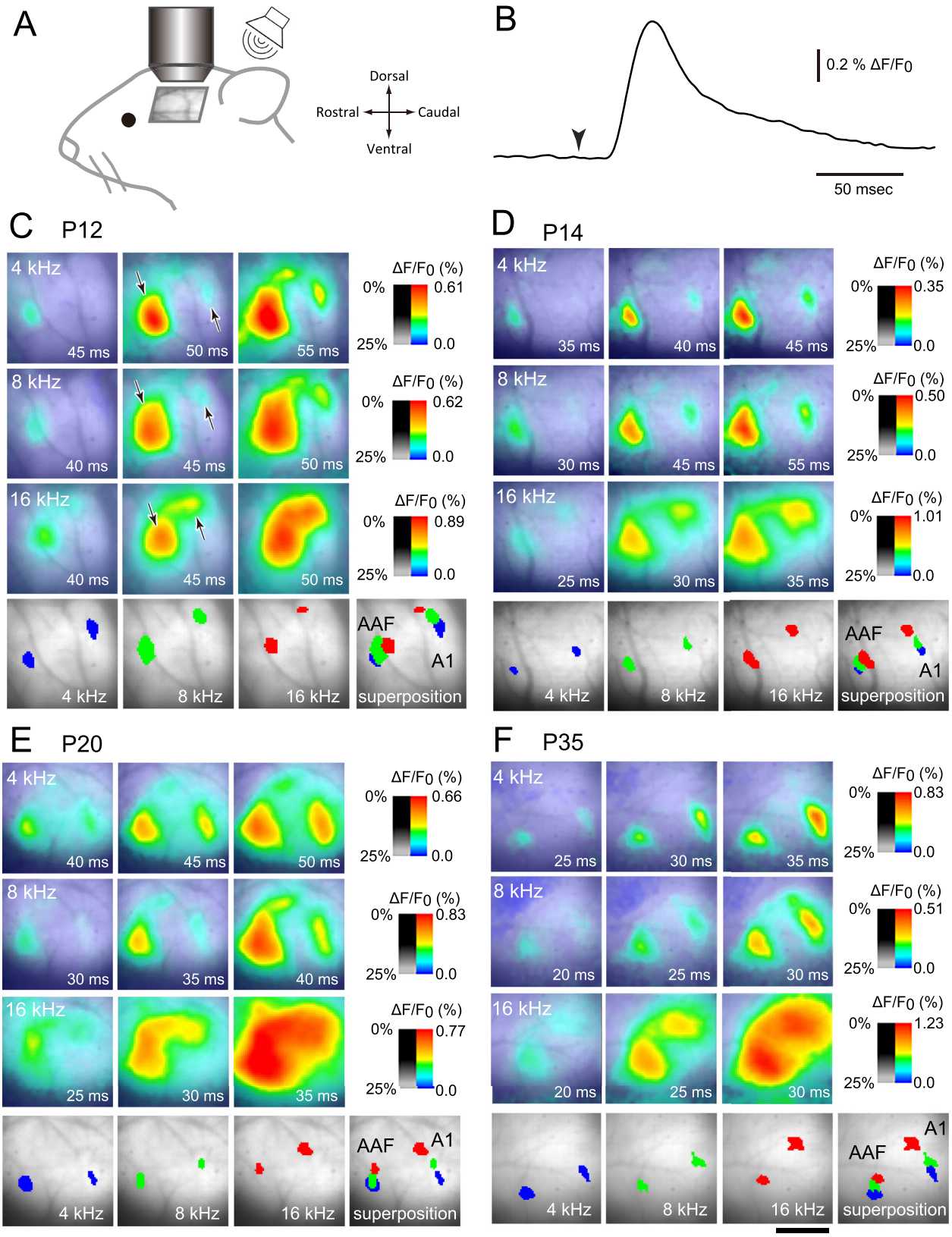

Fig. 1. Examples of optical recordings from mice at different postnatal ages. (A). Schematic drawing of optical recording (lens) from a neonatal mouse to acoustic stimulations (speaker). The auditory cortex in the left hemisphere was exposed and stained with the voltage-sensitive dye RH-1691. The orientation depicted on the right applies to all figures in this study. (B) The time course of a typical response ($\Delta F/F_0$) at one pixel, recorded from a P14 mouse. The arrowhead marks the onset of the tone stimulus, and time was counted in ms from the onset. (C) Average responses to 4- (top row), 8- (next to top row), and 16-kHz tones (next to bottom row) in a P12 mouse auditory cortex are color-encoded according to the color bar on the right and shown at the times illustrated at the bottom of each graph. The response was superimposed on the cortical basal fluorescence image, using the transparency bar shown on the right. The arrows mark initial responses at the rostral (AAF) and caudal sites (A1). The bottom row shows binarized onset responses to tones of 4- (blue), 8- (green), and 16-kHz (red). The superposition of the three onset responses (rightmost) revealed tonotopy in both A1 and AAF. (D-F) Results from mice at P14, P20, and P35, respectively, illustrated in the same way as in (C). Stimulus intensity was 60 dB SPL for 4- and 16-kHz tones in all figures; for 8 kHz tones, the intensity was 60 dB SPL in (C) and 30 dB SPL in other figures. The scale bar in (F) is 1 mm and applies to (C)-(E).

geometric centroid of the onset response to 4 kHz and 16 kHz was calculated and used to evaluate the size of A1 or AAF and the relative position between the subfields. A1 and AAF were identified using the frequency gradient determined by the onset responses to 4-, 8-, and 16-kHz tones, as in our previous studies (Sawatari et al., 2011; Takemoto et al., 2014; Nakata et al., 2020).

2.4. Statistics

Data are presented as the mean ± standard error of the mean (SEM). For each experimental condition, one recording was analyzed in one animal, and therefore the number of samples (n) is also the number of animals. Statistical significance was determined by the Wilcoxon signed-rank test for comparison between two groups (A1 vs. AAF, or high-frequency location vs. low-frequency location). The Kruskal–Wallis test was used to compare more than two groups (seven age groups), and the *post hoc* Tukey's test was used for multiple comparisons. The level of statistical significance was set at 0.05.

3. Results

3.1. Tonotopy in A1 and AAF from hearing onset

Tone-evoked activity in the auditory cortex was not found in mice at P11 ($n = 4$) for all frequencies tested (4, 8, and 16 kHz) at up to 80 dB SPL, but was successfully recorded from all P12 mice ($n = 4$) and all mice older than P12. An example of a tone-evoked response recorded from one channel from a P14 mouse is shown in Fig. 1B. The response rapidly reached a peak and then decayed with a longer time constant. The transient nature of the response is in accord with previous imaging studies using voltage-sensitive dyes in the adult auditory cortex (Horikawa et al., 2001; Song et al., 2006). To illustrate the spatiotemporal pattern of the response, we encoded the response amplitude at different times in the rise phase of the responses with color and superimposed the response onto the cortical surface image of basal voltage-sensitive dye fluorescence (Fig. 1C–F). Fig. 1C shows an example of recordings from a P12 mouse; responses to stimulations with 4- (top row), 8- (next to top row), and 16-kHz tones (next to bottom row) at three different times after tone onset (shown at the bottom of each graph) are illustrated. All tone stimuli were applied at 60 dB SPL. Each tone evoked early responses at 40–50 ms after stimulus onset at two sites: one in a rostral part and the other in a caudal part of the recorded field (Fig. 1C, arrows). Over time, the responses spread spatially to merge (data not shown). From Fig. 1C, the shift in the location of the caudal one along a dorsorostral direction with increasing tone frequency is obvious. To better illustrate the frequency-dependent shift of response location, tonotopy, we used an early onset response to a tone in each site (rostral and caudal), which was defined as the binarized response using a threshold of 20% of the maximum response (see Methods). The results of the onset response for the P12 mouse shown in Fig. 1C are depicted in the bottom row of the figure, with 4-, 8-, and 16-kHz onset responses in blue, green, and red, respectively. The superposition of the onset responses together revealed a clear trend of the shift toward the dorsorostral direction with increasing tone frequency for the caudal site, and a dorsocaudal shift for the rostral site (Fig. 1C, bottom row, rightmost graph). Based on the tonotopy in A1 and AAF reported in adult mice (Stiebler et al., 1997; Sawatari et al., 2011; Guo et al., 2012; Takemoto et al., 2014; Nakata et al., 2020), the rostral and caudal sites can be readily identified as AAF and A1, respectively. Similar observations were obtained in all four mice examined at P12. The same analyses applied to mice aged from P13 to P40 revealed similar results. Examples from mice aged at P14, P20, and P35, are shown in Fig. 1D–F, respectively. Our results suggest that both A1 and AAF exhibit tonotopy from the early onset of hearing.

3.2. Development of the size of A1 and AAF

Tonotopy has been quantitatively evaluated using CMF (Kalatsky et al., 2005; Storace et al., 2011; Mrsic-Flogel et al., 2006; Imaizumi and Schreiner, 2007; Nishimura and Song, 2014). To evaluate if tonotopy is subject to postnatal regulation, we first examined the postnatal development of the size of A1 and AAF, which will be used to calculate CMF in the following section. To this end, we measured the distance between the centroid of the onset response to 4 kHz and the centroid of the onset response to 16 kHz for both A1 (Fig. 2A) and AAF (Fig. 2B) in mice aged from P12 to P40. We refer to the distance in A1 or AAF as the size of the subfield, although this underestimates the actual size. As shown in Fig. 2A, the size of A1 increased rapidly from P12 to P14, and appeared to remain at a constant level after that. The mean values could be fitted with an exponential function with a time constant (τ) of 1.0 day ($r = 0.89$; Fig. 2A). Statistical analyses revealed significant differences among the age groups (Kruskal–Wallis test, $p = 0.005$), and a significant difference between the size at P12 and those at P20 and P35 (Tukey's *post hoc* test, $p < 0.05$).

Compared to the size of A1, the size of AAF appeared much smaller (Fig. 1C–F; also compare Fig. 2B to A); age-matched comparison between the two subfields revealed significant differences at all ages (Wilcoxon signed-rank test, $p = 0.03$, $n = 4$ for P12 and P13; $p = 0.008$, $n = 5$ for P14; $p = 0.008$, $n = 5$ for P20; $p = 0.03$, $n = 4$ for P26; P35 and P40 pooled together because of the small sample size at P35, $p < 0.0001$, $n = 8$). The size of AAF also changed to a lesser extent with age, compared to the change in A1 (Fig. 2B). Statistical analysis revealed a significant difference among age groups (Kruskal–Wallis test, $p = 0.03$), and a significant difference between P12 and P35 (Tukey's *post hoc* test, $p < 0.05$). The significant difference among age groups might be due to the large deviation of the P35 results from other results, but the data without P35 also had statistical significance (Kruskal–Wallis test, $p = 0.049$).

3.3. Development of tonotopy

To quantitatively examine the postanal development of tonotopy, we calculated CMF as the ratio of the frequency difference between 4 kHz and 16 kHz (2 octaves) to the size of A1 or AAF, as described above. As shown in Fig. 3A, the CMF in A1 appeared to decrease rapidly during P12–P14 and remained at a stable level after that. The mean values could be fitted with an exponential function with a time constant of 0.8 days and a plateau value of 3.36 octave/mm ($r = 0.94$). The statistical analysis revealed significant differences among the age groups (Kruskal–Wallis test, $p = 0.005$), and a significant difference between CMF at P12 and those at P20 and P35 (Tukey's *post hoc* test, $p < 0.05$).

Compared to A1, AAF appeared to have larger CMF values (compare Fig. 3B to A). Age-matched comparisons between the two subfields revealed significant differences at all ages (Wilcoxon signed-rank test, $p = 0.03$, $n = 4$ for P12 and P13; $p = 0.008$, $n = 5$ for P14; $p = 0.008$, $n = 5$ for P20; $p = 0.03$, $n = 4$ for P26; P35 and P40 pooled together, $p < 0.0001$, $n = 8$). Similar to CMF in A1, CMF in AAF also decreased rapidly from P12 and appeared to reach a stable level after the first two postanal weeks (Fig. 3B); the mean values could be fitted with an exponential function with a time constant of 1.4 days and a plateau value of 6.41 octave/mm ($r = 0.85$). Statistical analyses revealed significant differences among the age groups (Kruskal–Wallis test, $p = 0.03$), and a significant difference between the CMFs at P12 and P35 (Tukey's *post hoc* test, $p < 0.05$).

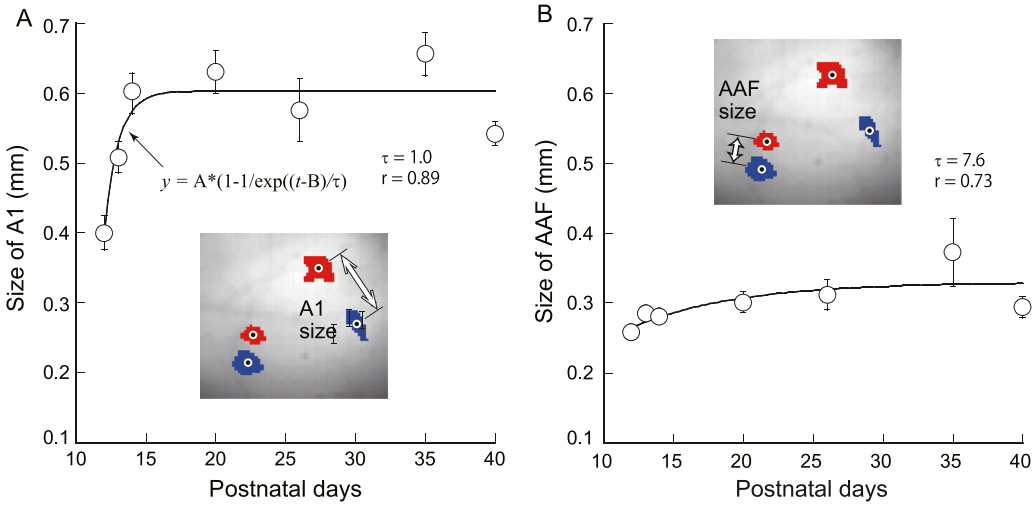

Fig. 2. Postnatal development of the size of A1 and AAF. (A) Postnatal development of the size of A1, evaluated using the distance between the centroid of the onset response to 4 kHz tones and that to 16 kHz tones (inset). The mean values at different ages were fitted with an exponential function in the form illustrated in the figure ($r = 0.89$), with a time constant of 1.0 days. Error bars are the SEM. Significant differences among the age groups ($p = 0.005$, Kruskal–Wallis test), as well as a significant difference between the size at P12 and those at P20 and P35 ($p < 0.05$, *post hoc* Tukey), were found. (B) Postnatal development of the size of AAF, evaluated again using the distance between the centroid of the onset response to 4 kHz and that to 16 kHz (inset). The mean values showed limited changes with age. The curve is the fitted curve using the same exponential function shown in (A). AAF size is significantly different from A1 size for all age groups (see text for detail).

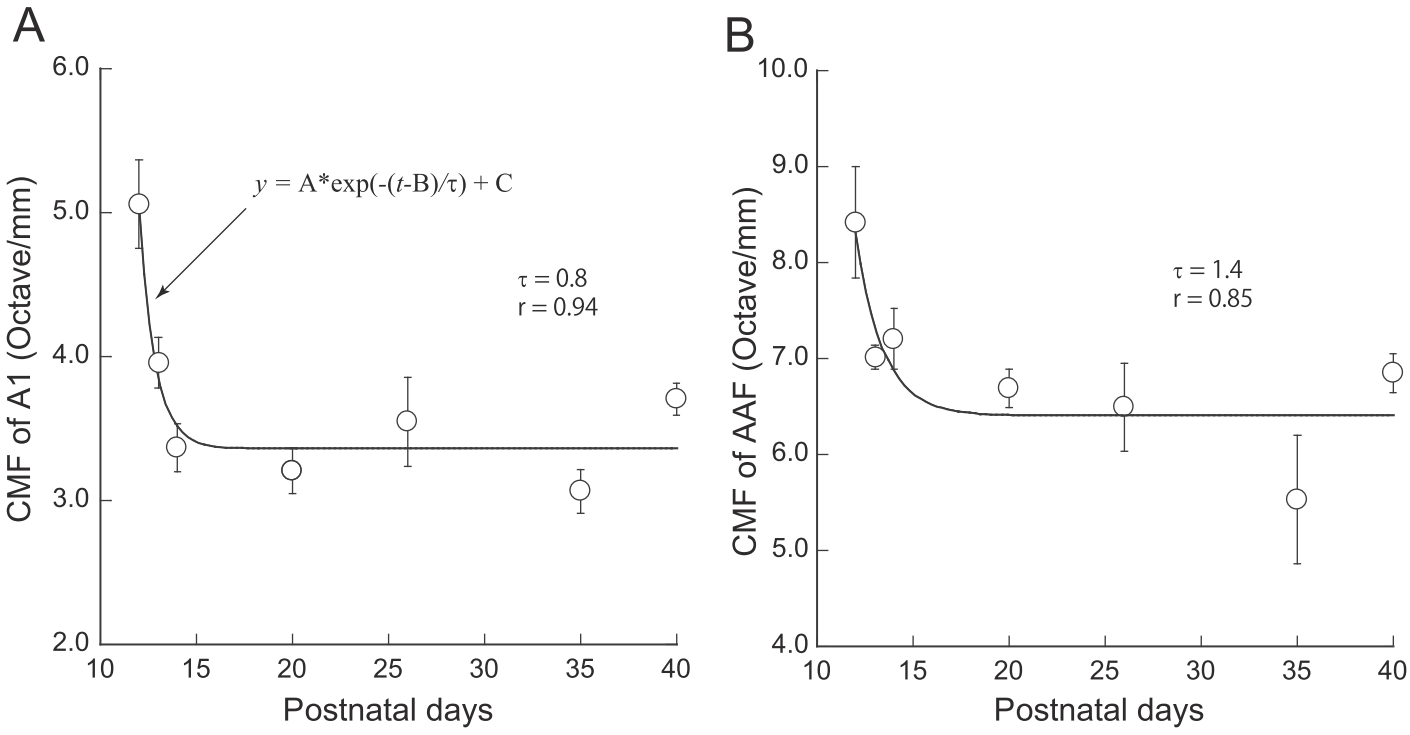

Fig. 3. Postnatal development of the cortical magnification factor (CMF) in A1 and AAF. CMF is the frequency difference between 16 kHz and 4 kHz in octaves, divided by the distance in mm between the centroids of the onset responses to the two frequencies in a subfield. (A) Postnatal development of CMF in A1. The mean values at different ages were fitted with an exponential function in the form illustrated in the figure ($r = 0.94$), with a time constant of 0.8 days. Significant differences among the age groups ($p = 0.005$, Kruskal–Wallis test), as well as a significant difference between the size at P12 and those at P20 and P35 ($p < 0.05$, *post hoc* Tukey), were found. (B) Postnatal development of CMF in AAF. The same exponential fit as in (A) resulted in a time constant of 1.4 days. Significant differences among the age groups ($p = 0.03$, Kruskal–Wallis test), as well as a significant difference between the size at P12 and that at P35 ($p < 0.05$, *post hoc* Tukey), were found. The pair-wise comparison between A1 and AAF at each age revealed significant differences in CMF (see text for detail).

The results described in this section suggest that tone frequency difference is progressively represented by a longer distance across the surface of both A1 and AAF between P12 to P14. The results also suggest a better spatial representation of frequency in A1 than in AAF.

3.4. Development of response properties

As one may notice in Fig. 1C–F, the response in younger animals appeared at a later time after the stimulus tone onset. To examine this developmental change, we measured the response la-

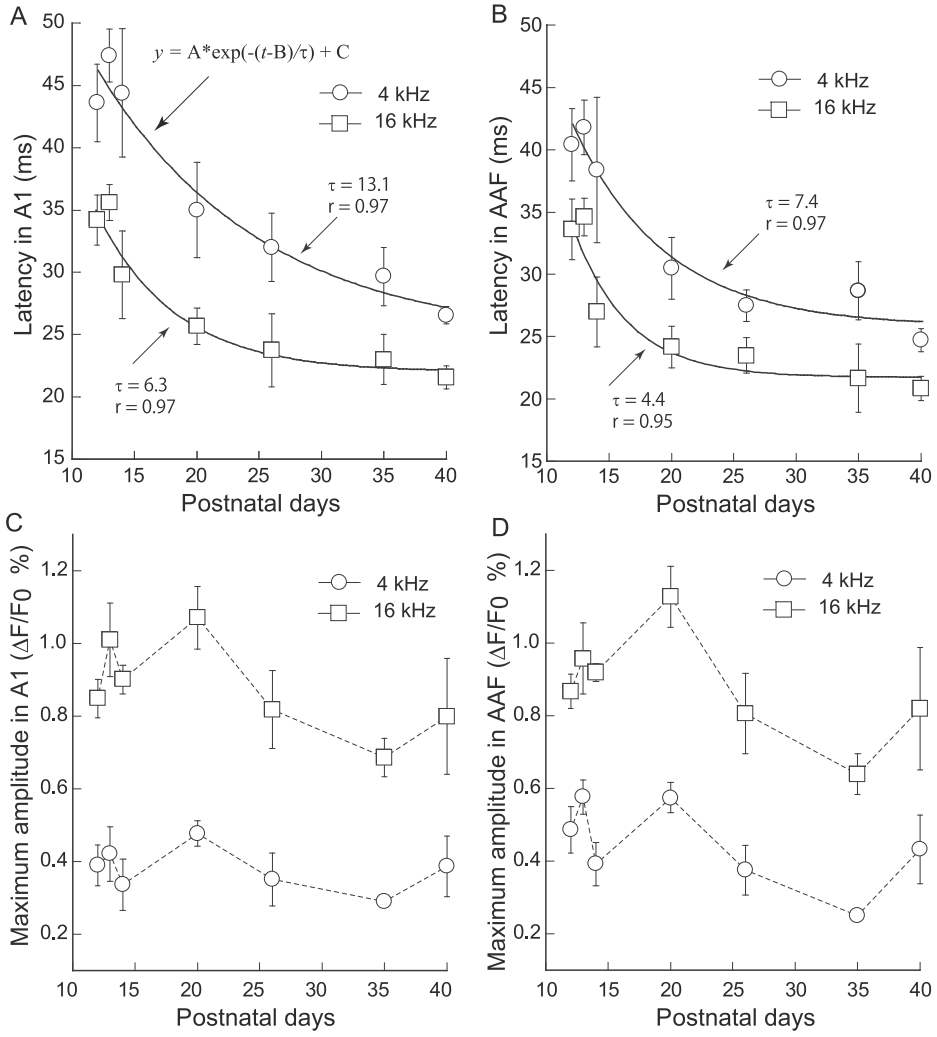

Fig. 4. Postnatal development of the frequency-dependent response latency and maximum response amplitude in A1 and AAF. (A) Postnatal development of the response latency to 4 kHz (circles) and 16 kHz tones (square) in A1. The mean values for both frequencies at different ages were fitted with an exponential function in the form illustrated in the figure ($r = 0.97$ for both 4 kHz and 16 kHz), with a time constant of 13.1 days for 4 kHz and 6.3 days for 16 kHz. Significant differences among the 4 kHz data groups ($p = 0.002$, Kruskal–Wallis test) and the 16 kHz groups ($p = 0.003$), a significant difference between the 4 kHz data at P12/P13/P14 and that at P40 ($p < 0.05$, *post hoc* Tukey), and a significant difference between the 16 kHz data at P12/P13 and that at P40 for ($p < 0.05$) were found. The pair-wise comparison between latencies to 4 kHz and 16 kHz tones at each age revealed significant differences (see text for detail). (B) Postnatal development of response latency to 4 kHz tone (circles) and 16 kHz tones (square) in AAF. The mean values for both frequencies at different ages were fitted with an exponential function as in (A) ($r = 0.97$ for 4 kHz and $r = 0.95$ for 16 kHz), with a time constant of 7.4 days for 4 kHz and a time constant of 4.4 days for 16 kHz. Significant difference among the 4 kHz data groups ($p = 0.002$, Kruskal–Wallis test) and the 16 kHz groups ($p = 0.004$), a significant difference between the 4 kHz data at P12/P13 and that at P40 ($p < 0.05$, *post hoc* Tukey), and a significant difference between the 16 kHz data at P12/P13 and that at P40 for ($p < 0.05$) were found. The pair-wise comparison between latencies to 4 kHz and 16 kHz tones at each age revealed significant differences for all ages (see text for detail). (C) The postnatal development of the maximum response amplitude to 4 kHz (circles) and 16 kHz tones (square) in A1. No significant differences among the 4 kHz ($p = 0.61$, Kruskal–Wallis test) or 16 kHz groups ($p = 0.26$) were found. The pair-wise comparison between the maximum amplitude of responses to 4 kHz and 16 kHz tones at each age revealed significant differences for all ages (see text for detail). (D) Postnatal development of the maximum response amplitude to 4 kHz (circles) and 16 kHz tones (square) in AAF. No significant differences among the 4 kHz ($p = 0.26$, Kruskal–Wallis test) or 16 kHz groups ($p = 0.12$) were found. The pair-wise comparison between the maximum amplitude of responses to 4 kHz and 16 kHz tones at each age revealed significant differences for all ages (see text for detail).

tency as the interval from the stimulus onset to when the response exceeded three times the baseline SD (see Methods). We defined the latency of A1 or AAF as the latency of the pixel showing the largest peak in the subfield. Results of response latency in A1 to 4- and 16-kHz tones, all applied at 60 dB SPL, are shown in Fig. 4A. In contrast to the rapid change of CMF only during P12–P14, response latency showed limited change during this period, but became progressively shorter over the entire postnatal period examined (P12–P40; Fig. 4A). The mean values at different ages decreased exponentially with a time constant of 13.1 days for responses evoked by 4 kHz tones (Fig. 4A, upper curve), and a time constant of 6.3 days for responses evoked by 16 kHz tones (Fig. 4A, the lower curve), suggesting that the response to 16 kHz tones matured faster than the response to 4 kHz tones. Statistical analyses revealed significant differences in the latencies of responses to both 4 kHz tones (Kruskal–Wallis test, $p = 0.002$) and 16 kHz tones ($p = 0.003$), significant differences between the latency at P12/P13/14 and that at P40 (Tukey's *post hoc* test, $p < 0.05$) for the responses to 4 kHz tones, and significant differences between the latency at P12/P13 and that at P40 ($p < 0.05$) for the responses to 16 kHz tones. As shown in Fig. 4A, the latencies of responses to 16 kHz tones appeared shorter than the latencies of responses to 4 kHz tones. An age-matched comparison between the two frequencies revealed significant differences at all ages (Wilcoxon signed-rank test, P12–P14 pooled together, $p < 0.0001$, $n = 15$; P20–P26 pooled together, $p = 0.004$, $n = 10$; P35–P40 pooled together, $p = 0.004$, $n = 10$).

Similar results were obtained for AAF (Fig. 4B). The mean values at different ages decreased exponentially with a time constant

of 7.4 days for responses evoked by 4 kHz tones (Fig. 4B, the upper curve), and a time constant of 4.4 days for responses evoked by 16 kHz tones (Fig. 4B, the lower curve), again suggesting that the response to 16 kHz tones matured faster than the response to 4 kHz tones. A Kruskal–Wallis test and *post hoc* Tukey analysis revealed significant differences in the latencies of responses to both 4 kHz tones ($p = 0.002$) and 16 kHz tones ($p = 0.004$), and a significant difference between the latency at P12/P13 and that at P40 ($p < 0.05$) for responses to both tones. Similar to the case of A1, the latencies of responses to 16 kHz in AAF also appeared shorter than the latencies of responses to 4 kHz. An age-matched comparison between the two frequencies revealed significant differences at all ages (Wilcoxon signed-rank test, P12–P14 pooled together, $p < 0.001$, $n = 15$; P20–P26 pooled together, $p = 0.008$, $n = 10$; P35–P40 pooled together, $p = 0.008$, $n = 10$).

The latency appeared smaller in AAF than in A1 (Fig. 4A and B). Frequency- and age-matched comparisons between the two subfields revealed statistical significance for responses evoked by 4 kHz tones (Wilcoxon signed-rank test, P12–P14 pooled together, $p < 0.001$, $n = 15$; P20–26 pooled together, $p = 0.008$, $n = 10$; P35–P40 pooled together, $p = 0.02$, $n = 10$), but no significance for responses evoked by 16 kHz (Wilcoxon signed-rank test, P12–P14 pooled together, $p = 0.12$, $n = 15$; P20–P26 pooled together, $p = 0.25$, $n = 10$; P35–P40 pooled together, $p = 0.11$, $n = 10$).

From Fig. 1C–F, the magnitude of the response in AAF appears larger than that in A1. To test this notion, we measured the maximum response amplitude in both A1 and AAF for tones evoked by 4- and 16-kHz tones, all applied at 60 dB SPL, at different ages (Fig. 4C and D). No statistical significance was found among the age groups ($p = 0.26$ and $p = 0.61$ for maximum responses to 4 kHz and 16 kHz tones, respectively, in A1; $p = 0.26$ and $p = 0.12$ for maximum responses to 4 kHz and 16 kHz tones, respectively, in the AAF; Kruskal–Wallis test). However, the maximum response to 16 kHz tones appeared to be larger than that to 4 kHz tones in both A1 and AAF (Fig. 4C and D); an age-matched comparison between the two frequencies revealed significant differences at all ages for both subfields (A1 and AAF: Wilcoxon signed-rank test, $p < 0.0001$, $n = 15$ for P12–P14 pooled together; $p = 0.004$, $n = 10$ for P20–P26 pooled together; $p = 0.004$, $n = 10$ for P35–P40 pooled together).

Previous studies have reported faster temporal responses in AAF compared with A1 in cats (Schreiner and Urbas, 1988), rats (Polley et al., 2007), and mice (Linden et al., 2003; Sołyga and Barkat, 2019). To examine if a similar difference can be revealed using our optical signal and how the difference is regulated over postnatal development, we measured and compared the rise time and duration of responses evoked by 4- and 16-kHz tones, both applied at 60 dB SPL, in A1 and AAF. Rise time was defined as the time for the response in the pixel showing the largest peak in the subfield to rise from 20% to 80% of the peak value in the rise phase, and duration was defined as the response duration at 50% of the peak value in the same pixel. We found no significant difference between A1 and AAF in either rise time or duration, at all ages examined (Wilcoxon signed-rank test. Rise time: 4 kHz tones, $p > 0.22$ for all age groups; 16 kHz tones, $p > 0.54$ for all age groups. Duration: 4 kHz tones, $p > 0.29$ for all age groups; 16 kHz tones, $p > 0.17$ for all age groups. Fig. 5). For the rise time, we found no significant difference among the age groups for responses evoked by both tones, in either A1 and AAF (Fig. 5A and B; Kruskal–Wallis test, A1: $p = 0.31$ for 4 kHz and $p = 0.76$ for 16 kHz; AAF: $p = 0.30$ for 4 kHz and $p = 0.06$ for 16 kHz). For the duration, we found no significant difference among the age groups for responses evoked by 4 kHz tones, in either A1 and AAF (Fig. 5C and D; Kruskal–Wallis test, $p = 0.26$ for A1 and $p = 0.33$ for AAF), but significant difference among the age groups for responses evoked by 16 kHz tones, in both A1 and AAF (Fig. 5C and D; Kruskal–Wallis test, $p = 0.002$ for A1 and $p = 0.001$ for AAF). The duration of responses evoked by 16 kHz tones decreased exponentially with postnatal development in both A1 and AAF (Fig. 5C and D). Frequency-dependent difference in both rise time and duration was also found in both A1 and AAF (Wilcoxon signed-rank test; rise time in A1: $p = 0.08$, $n = 15$ for P12–P14 pooled together; $p = 0.01$, $n = 10$ for P20–P26 pooled together; $p = 0.04$, $n = 10$ for P35–P40 pooled together; rise time in AAF: $p = 0.41$, $n = 15$ for P12–P14 pooled together; $p = 0.03$, $n = 10$ for P20–P26 pooled together; $p = 0.02$, $n = 10$ for P35–P40 pooled together; duration in both A1 and AAF: $p < 0.04$ for all age groups; Fig. 5)

Previous studies have also reported that AAF neurons have broader frequency tuning than A1 neurons in mice (Hackett et al., 2011; Guo et al., 2012) and cats (Imaizumi et al., 2004). If this is the case in neonatal mice, a pure tone is expected to activate a larger cortical area in AAF than in A1; it is also of interest if this difference between A1 and AAF arises during postnatal development. To test these points, we compared the area activated by a 4 kHz tone at 60 dB SPL in A1 and AAF over postnatal development; the activated area was defined using a threshold of 50% of the subfield's maximum response. The ratios of activated area in AAF over the area in A1 were 2.75 ± 0.48 at P12, 4.41 ± 2.26 at P13, 3.53 ± 1.37 at P14, 2.79 ± 0.75 at P20, 2.59 ± 1.15 at P26, 4.33 ± 1.97 at P35, and 3.24 ± 0.58 at P40. The larger than one mean values at all ages are in line with the previous reports of broader frequency tuning in AAF than in A1, but no significant difference was found among the age groups (Kruskal–Wallis test, $p = 0.96$).

3.5. Development of the relative position between A1 and AAF

Our wide-field imaging of A1 and AAF at the same time allowed us to examine how the relative position between A1 and AAF develops with age. For this purpose, we measured the distance between the centroid of the onset response to 4 kHz in A1 and AAF (referred to as D4), as well as the distance between the centroid of onset response to 16 kHz in A1 and AAF (referred to as D16; Fig. 6A). Similar to the size of the subfields, both D4 and D16 increased rapidly during the narrow period of P12–P14. The mean values of D4 and D16 at different ages increased exponentially, with a time constant of 1.4 days for D4 and 1.8 days for D16 (Fig. 6A). Statistical analyses revealed significant differences for D4 (Kruskal–Wallis test, $p = 0.003$) and D16 (Kruskal–Wallis test, $p = 0.002$), a significant difference between D4 at P12/P13 and that at P20 (Tukey's *post hoc* test, $p < 0.05$), and a significant difference between D16 at P12 and those at P20 and P40 (Tukey's *post hoc* test, $p < 0.05$). It is also clear from Fig. 6A that D4 appeared to be larger than D16 at all ages. An age-matched comparison between the two distances revealed significant differences at all ages (Wilcoxon signed-rank test, P12–13 pooled together, $p = 0.008$, $n = 8$; P14–20 pooled together, $p = 0.002$, $n = 10$; P26–40 pooled together, $p < 0.0001$, $n = 12$).

The extent of the age-dependent increase of D4 appeared to be smaller than that of D16. D4 increased from an average value of 1.14 mm ($n = 4$) at P12 to a plateau value of 1.37 mm, derived from the exponential fit (Fig. 6A). The difference (0.23 mm) is much smaller than the difference of 0.35 mm calculated for D16 (0.69 mm at P12, and the exponential plateau of 1.04 mm). This differential regulation by development can also be appreciated by calculating the angle between the frequency axis of A1 and that of AAF. We defined the line connecting the centroid of the onset response to 4 kHz and that to 16 kHz in A1 or AAF as the frequency axis of the subfield. As shown in Fig. 6B, the angle showed a rapid initial decrease, and appeared to remain at a stable value after two weeks postnatal. The mean values at different ages were best fitted with an exponential function having a time constant of 1.8 days

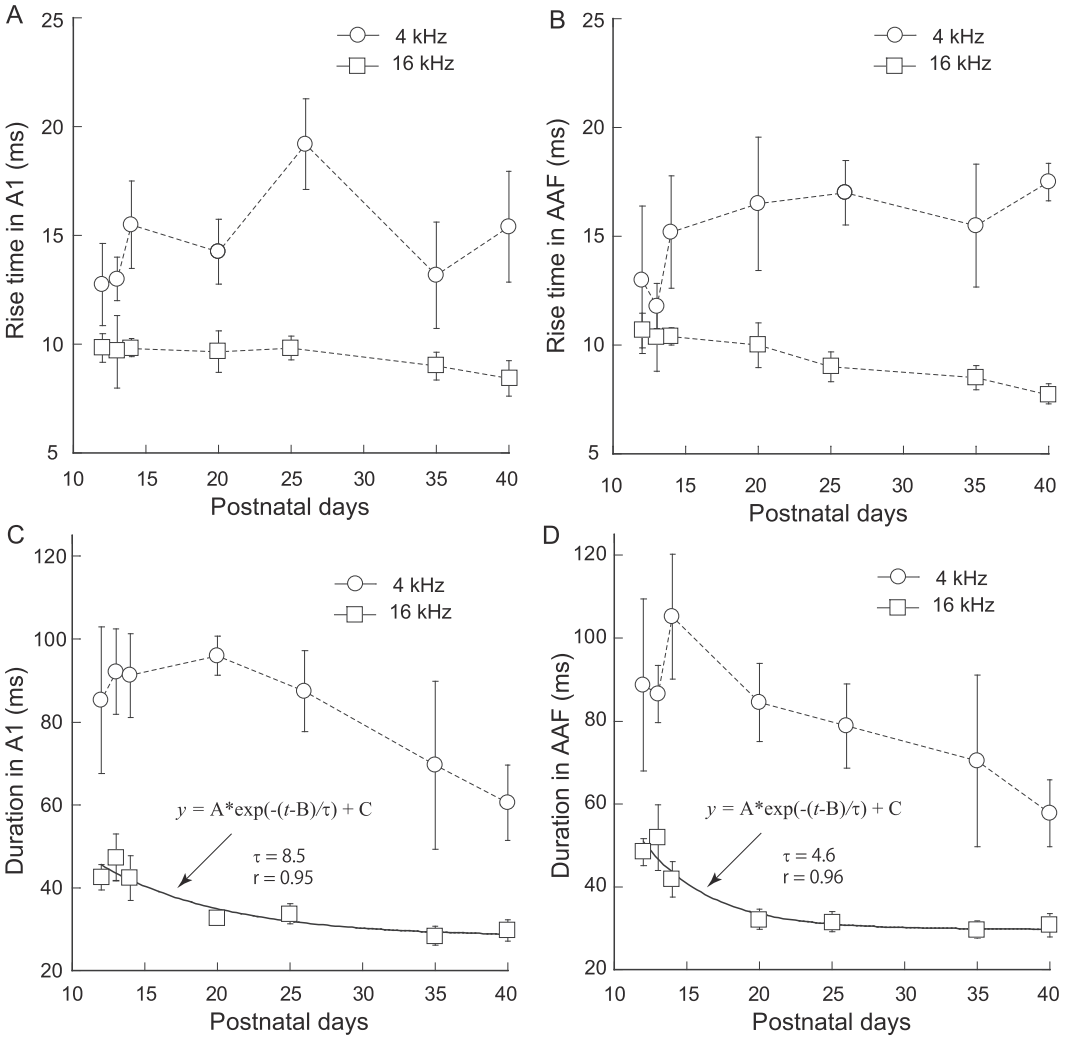

Fig. 5. Postnatal development of response rise time and duration in A1 and AAF. (A) Postnatal development of the rise time of response to 4- (circles) and 16-kHz (square) tones in A1. No significant difference was found among the age groups for both tones ($p = 0.31$ for the 4 kHz data and $p = 0.76$ for the 16 kHz data, Kruskal–Wallis test). Frequency-dependent difference in rise time was not found for younger animals (Wilcoxon signed-rank test; $p = 0.08$, $n = 15$ for P12-P14 pooled together), but was found in older animals ($p = 0.01$, $n = 10$ for P20-P26 pooled together; $p = 0.04$, $n = 10$ for P35-P40 pooled together). (B) Postnatal development of the rise time of response to 4- (circles) and 16-kHz (square) tones in AAF. No significant difference was found among the age groups for both tones ($p = 0.30$ for the 4 kHz data and $p = 0.06$ for the 16 kHz data, Kruskal–Wallis test). Frequency-dependent difference in rise time was not found for younger animals (Wilcoxon signed-rank test; $p = 0.41$, $n = 15$ for P12-P14 pooled together), but was found in older animals ($p = 0.03$, $n = 10$ for P20-P26 pooled together; $p = 0.02$, $n = 10$ for P35-P40 pooled together). (C) Postnatal development of the duration of responses to 4- (circles) and 16-kHz (square) tones in A1. No significant difference was found among the 4 kHz data groups ($p = 0.26$, Kruskal–Wallis test), but a significant difference was found for the 16 kHz data groups ($p = 0.002$) which could be fitted with an exponential function as depicted in the figure. Frequency-dependent difference in duration was found for all age groups (Wilcoxon signed-rank test; $p < 0.04$ for all age groups). (D) Postnatal development of the duration of response to 4- (circles) and 16-kHz (square) tones in AAF. No significant difference was found among the 4 kHz data groups ($p = 0.33$, Kruskal–Wallis test), but a significant difference was found for the 16 kHz data groups ($p = 0.001$) which could be fitted with an exponential function as depicted in the figure. Frequency-dependent difference in duration was found for all age groups (Wilcoxon signed-rank test; $p < 0.04$ for all age groups). Comparison between A1 and AAF in either rise time or duration revealed no significant difference at all ages examined (Wilcoxon signed-rank test. Rise time: 4 kHz tones, $p > 0.22$ for age groups; 16 kHz tones, $p > 0.54$ for age groups. Duration: 4 kHz tones, $p > 0.29$ for age groups; 16 kHz tones, $p > 0.17$ for age groups).

and a stable value of 61.6° (r = 0.99). Statistical analyses revealed significant differences among the age groups (Kruskal–Wallis test, $p = 0.03$), a significant difference between the angle at P12 and those at P20, P26, and P40 (Tukey's *post hoc* test, $p < 0.05$), and a significant difference between the angles at P13 and P20 (Tukey's *post hoc* test, $p < 0.05$).

4. Discussion

Here we have found 1) that both AAF and A1 exhibited tonotopy from hearing onset, and that tonotopy developed rapidly in terms of CMF toward the end of the second postnatal week, 2) that the size of both subfields and the relative position between the two subfields developed in a time course similar to that of CMF, and 3) that the latency and duration of tone-evoked responses (duration of only16-kHz-tone evoked responses) in the subfields decreased slowly during the first postnatal month. These observations can be summarized as two postnatal developmental processes: a fast process occurring mainly during P12–P14, manifested as the change in CMF, D4, D16, and the angle between the frequency axis of A1 and AAF, and a slow process during the first postnatal month, manifested as the shortening of response latency and duration in both A1 and AAF.

4.1. Development of tonotopy

One major finding of the current study is that tonotopy is observed in both A1 and AAF from the early onset of hearing

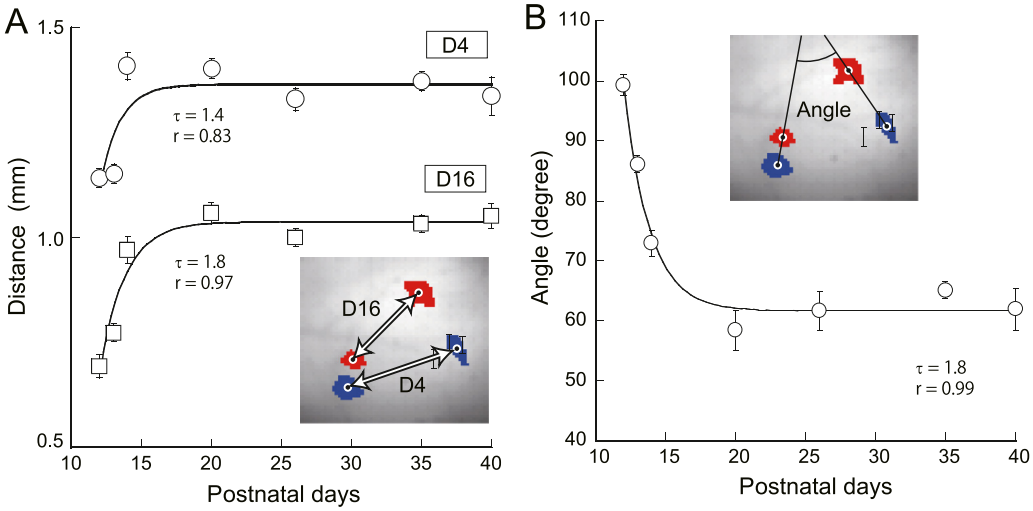

Fig. 6. Postnatal development of the positional relationship between A1 and AAF. (A) The distance between A1 and AAF at the low-frequency region was evaluated by measuring the distance between centroids of the onset responses to 4 kHz in A1 and AAF (D4, inset; data shown in circles). The distance at the high-frequency region was evaluated by the distance between the centroids of the onset responses to 16 kHz in A1 and AAF (D16, inset; data shown in squares). The mean values of both D4 and D16 were fitted with an exponential function ($r = 0.83$ for D4 and $r = 0.97$ for D16), with a time constant of 1.4 days for D4 and 1.8 days for D16. Significant differences among the D4 data ($p = 0.003$, Kruskal–Wallis test) and D16 data groups ($p = 0.002$, Kruskal–Wallis test), a significant difference between the D4 values at P12/P13 and those at P20 ($p < 0.05$, *post hoc* Tukey), and a significant difference between the D16 values at P12 and those at P20/P40 ($p < 0.05$, *post hoc* Tukey) were found. The pair-wise comparison between D4 and D16 at each age revealed a significant difference for all ages (see text for detail). (B) Postnatal development of the angle between the frequency axis of A1 and AAF. The frequency axis is defined as the line connecting the centroid of onset response to 4 kHz and 16 kHz tones in A1 or AAF (inset). The mean values of the angle were fitted with an exponential function ($r = 0.99$, time constant = 1.8 days). Significant differences among the angle data groups ($p = 0.03$, Kruskal–Wallis test), a significant difference between the angle data at P12 and that at P20, P26, and P40 ($p < 0.05$, *post hoc* Tukey), and a significant difference between the angle at P13 and that at P20 ($p < 0.05$, *post hoc* Tukey) were found.

(P12) in mice. It has been reported recently that tonotopic spontaneous activity occurs at several auditory centers, including the auditory cortex, before hearing onset in mice (Babola et al., 2018). These findings suggest that tonotopy in the mouse core region of the auditory cortex is formed primarily by genetic mechanisms, although a role of spontaneous activities has also been discussed (Babola et al., 2018; reviewed in Wang and Bergles, 2015). Tonotopy is created in the cochlea and must be preserved along the ascending auditory pathway in order for the cortex to exhibit tonotopy (Liberman, 1982; Nishimura and Song, 2014; reviewed in Pickles, 2008). A1 and AAF have been shown in mice to receive distinct, topographic inputs from the auditory thalamus (Horie et al., 2013; Takemoto et al., 2014). Therefore, it is likely that genetic mechanisms operate in parallel auditory ascending pathways to yield tonotopy in both A1 and AAF from early hearing onset. The hearing onset shown here (P12) is a day later than that shown electrophysiologically in previous rat and mouse studies (Geal-Dor et al., 1993; de Villers-Sidani et al., 2007; Polley et al., 2013). This difference might be attributable to the lower sensitivity of our imaging method or the strain difference in mice (ICR vs CBA/CaJ). The sudden appearance of tone-evoked response at P12 in the present study may in part be attributable to maturation of the middle ear. A previous rat study has reported that auditory brainstem response can be observed 3-4 days earlier for bone-conducted stimuli (at P7-8) than for air-conducted stimuli (at P11) and that the air-conduction mechanism maturates only by P15 (Geal-Dor et al., 1993).

We have further shown in the current study that tonotopy in both A1 and AAF exhibited a rapid quantitative change during P12–P14. Specifically, the cortical unit distance represented progressively smaller frequency differences during this period in both A1 and AAF, as demonstrated using the CMF index. Developmental changes in CMF depend on the change in cortical size. The time course of change in the size of A1 found here is in agreement with a previous finding in rats (de Villers-Sidani et al., 2007). Here, we have shown that the sizes of A1 and AAF developed in parallel. The CMF values identified here in A1, despite the developmental changes, fall within the range reported previously in rodents (1.4–5.0 octave/mm; Kalatsky et al., 2005; Mrsic-Flogel et al., 2006; Storace et al., 2011). We speculate two alternative mechanisms for the rapid changes in CMF in A1 and AAF during P12-P14. One is that the cortex does not change, but the thalamic input shifts its innervation position to yield changes in CMF, and the other is that A1 and AAF expand during P12–P14, and the thalamic input position shifts passively accompanying the cortical expansion. As thalamic axons tend to ramify axonal arbors locally once they enter the cortical plate (reviewed in Yamamoto, 2002), the former is less likely than the latter. Although the bulk of neurogenesis occurs during the embryonic period (reviewed in Cadwell et al., 2019), the rodent brain and cerebral cortex also undergo a significant postnatal expansion. The mouse brain volume is less than 20% of the adult volume at birth but increases rapidly during the first three postnatal weeks to approach the adult volume at about P20 (Kobayashi, 1963; Baloch et al., 2009; Chuang et al., 2011). Brain growth spurt in rats occurs from birth to two weeks postpartum (Dobbing and Sands, 1971). Therefore, the rapid change in CMF during P12–P14 observed here is most likely attributable to the expansion of the auditory cortex. The reduction of the angle between the frequency axis of A1 and that of AAF further suggests more expansion in the dorsal part of the auditory cortex than in the ventral part.

CMF values in A1 were smaller than those in AAF (see Fig. 3). A smaller CMF value indicates a unit cortical distance (area) for a smaller frequency difference, namely, a higher spatial resolution of frequency. Therefore, our findings are consistent with the idea that AAF is more involved in temporal processing, whereas A1 favors spectral processing (Hackett et al., 2011; Guo et al., 2012; Polley et al., 2007; Linden et al., 2003; Sołyga and Barkat, 2019).

The frequency gradients in A1 and AAF shown here at all ages are in agreement with those shown in adult mice in previous electrophysiological (Stiebler et al., 1997; Hackett et al., 2011; Guo et al., 2012) and real-time imaging studies (Sawatari et al.,

2011; Takemoto et al., 2014; Nakata et al., 2020), but in disagreement with imaging techniques that exploit Ca^{2+} signals or flavo-protein signals (Issa et al., 2014; Takahashi et al., 2006; Kubota et al., 2008). Instead of a dorsal shift of response location with increasing tone frequency in A1 and AAF, the latter studies reported a ventral shift in both subfields. The reason for this discrepancy is unclear, but it is clear that Ca^{2+} signals and flavo-protein signals are slow signals but neuronal spikes and voltage-sensitive dye signals are fast real-time signals. To a tone stimulation, cortical neurons can show an ON-response, an OFF-response, and some late responses at more than 200 ms after tone onset (Chen et al., 2015). Tonotopy has always been evaluated using the ON-response, with latencies less than 50 ms, in electrophysiological studies in mice (Stiebler et al., 1997; Guo et al., 2012) and other species (reviewed in Pickles, 2008). The OFF-response frequency selectivity is drastically different from that of the ON-response in the same cell (Sollini et al., 2018; Sołyga and Barkat, 2019). The onset response of optical signals analyzed here and in our previous studies have latencies less than 50 ms. We speculate that the discrepancy described above is largely attributable to the difference in time of response measurement (within 50 ms after stimulus onset in electrophysiological and real-time imaging studies; 400 ms or 500 ms in Ca^{2+} and flavo-protein studies).

The experience-dependent modification of the tonotopic map has been well documented in A1 of rats (Bao et al., 2001; de Villers-Sidani et al., 2007) and mice (Barkat et al., 2011; Polley et al., 2013). Exposure to a pure tone during a critical period causes persistent expansion of the area in A1 having a characteristic frequency of the tone (reviewed in Hensch, 2005; Keuroghlian and Knudsen, 2007; Sanes and Bao, 2009). The critical period is P12–P15 in mice (Barkat et al., 2011). Interestingly, this period coincides with the period of rapid CMF change shown in the current study. It is also interesting that the end of the critical period is when the CMF and the relative position between A1 and AAF reach a stable level (see Figs. 3 and 6). Future studies should examine if tone exposure causes changes in the frequency map in AAF and the relative position between A1 and AAF. So far, sound exposure has not been reported to affect AAF (Takahashi et al., 2006; Reinhard et al., 2019; cf. Meredith and Lomber, 2011).

4.2. Development of temporal response properties

We found here that response latency in both A1 and AAF decreased much more slowly (time constant $>$ 4 days) during postnatal development, compared with the changes in CMF and the relative position between A1 and AAF (time constant $<$ 2 days). The response latency in the auditory cortex depends on the electrophysiological properties of the entire ascending auditory pathway, and the postnatal change should be determined primarily by two factors: action potential conduction velocity of axons along the pathway, and synaptic integration time to reach the threshold at each stage of the pathway. It has been shown in early studies that myelination of thalamocortical fibers in rodents begins only at P14–P17 (Jacobson, 1963) and that the myelination rate reaches its peak at about P20 (reviewed in Semple et al., 2013). These facts predict a slow reduction of response latency in the cortex over the first postnatal month, considering that myelination is a major factor in reducing action potential conduction time. Concerning synaptic integration, it has been shown that synaptogenesis in rodents begins *in utero* but continues for the first three weeks postnatally (reviewed in Watson et al., 2006). Synaptic bouton distribution in the auditory brainstem shows drastic changes during the third postnatal week (Clause et al., 2014). The size and shape of synaptic potentials recorded, excitation and inhibition correlation as well as cellular electrophysiological properties also develop in rodent A1 over the first postnatal month (Aramakis et al., 2000; Oswald and Reyes, 2011; Froemke and Jones, 2011). Therefore, it is reasonable to speculate that both myelination and maturation of synaptic function along the auditory pathway contribute to the shortening of the response delays observed in the present study.

Our results also showed that the response latency to a high-frequency tone (16 kHz) was shorter than that to a low-frequency tone (4 kHz), in both A1 and AAF, at all ages examined (see Fig. 4). The difference was as large as 10 ms in A1 during the second and the third postnatal week but reduced to about 5 ms at P40 (see Fig. 4A). The reason for this difference is unclear, but it could be a functional feature of frequency-specific, parallel pathways of the ascending auditory circuits, as we have discussed in the section on the development of tonotopy. Another interesting observation is that the latency of response to the high-frequency tone (16 kHz) decreased faster with postnatal development than the latency to the low-frequency tone (4 kHz), in both A1 and AAF (see Fig. 4). These observations suggest faster functional maturation of the high-frequency region (dorsal A1 and dorsal AAF) than the low-frequency region (ventral A1 and ventral AAF). However, the maturation should include subcortical structures as well. This notion is in agreement with a recent finding of the dorsal-to-ventral maturation of the entorhinal cortex in rats (Ray and Brecht, 2016).

In the current study, we found no significant difference in response rise time and duration between A1 and AAF (see Fig. 5). This observation should not be taken as evidence against previous reports of faster temporal responses in AAF (Schreiner and Urbas, 1988; Linden et al., 2003; Polley et al., 2007; Sołyga and Barkat, 2019), because how our optical signal relates with neuronal spike activities is unknown (see the following section for discussion). In the present study, we found an exponential decrease in the duration of responses to 16 kHz tones, in both A1 and AAF (time constant $>$ 4 days; see Fig. 5). Tone-evoked responses in the auditory cortex have both glutamatergic excitatory components and GABAergic inhibitory components (Horikawa et al., 1996). Postnatal reduction of response duration should at least in part be attributable to the development of inhibitory circuits in the auditory cortex. We also found in the current study that the responses to 16 kHz tones had shorter durations than the responses to 4 kHz tones (see Fig. 5C and D), suggesting faster temporal processing in the high frequency region of the cortex.

4.3. Limitations of the current study

Although our imaging method has the advantage of recording from both A1 and AAF simultaneously with high temporal and spatial resolutions, there are several limitations to our study. First, because sound frequency is represented in a two-dimensional sheet in the auditory cortex, the geometrical indices used here including the CMF, do not fully capture the spatial representation of sound in the cortex. A frequency is usually represented by a strip of the cortex, defined by the cluster of neurons having the same characteristic frequency (Stiebler et al., 1997; Zhang et al., 2001; Guo et al., 2012; Polley et al., 2013), but here we used only one point, i.e., the centroid of onset response, for one frequency. Second, it is not clear how the onset response defined here relates to the characteristic frequency. However, the tonotopy defined using the onset response agrees well with those defined by characteristic frequencies in different species (Song et al., 2006; Sawatari et al., 2011; Takemoto et al., 2012; Nishimura and Song, 2014; Nishimura et al., 2018; Nakata et al., 2020). Finally, it is unclear how optical signals relate to neuronal spike activities. Because voltage-sensitive dye imaging signals resemble field potentials (Grinvald et al., 1994; Tokioka et al., 2000), the signal should depend on thalamic synaptic inputs, in addition to spike activities in the cortex. The larger amplitude of response to 16 kHz than 4 kHz tones found here (see Fig. 4C and D) may reflect the lower threshold of cortical neurons

to 16 kHz tones (de Villers-Sidani et al., 2007; Polley et al., 2013), but the exact relationship between our $\Delta F/F_0$ signal and neuronal firing rate is unknown. Despite the limitations listed here, our results provide new insights into the development of tonotopy and temporal response properties in A1 and AAF and the relative position between A1 and AAF.

5. Conclusions

In conclusion, both A1 and AAF exhibited tonotopy at hearing onset, and the tonotopy in the two subfields developed in parallel postnatally, showing rapid maturation toward the end of the second postnatal week. The relative position between the two subfields also maturated in the same time course. Response latency and duration in both A1 and AAF matured during the first postnatal month, with a faster maturation in the dorsal part of both subfields.

Author statement

F.C. and W.-J.S. designed the study; F.C., M.T., M.N., and R.T. collected data; F.C. and W.-J.S. analyzed data, prepared figures, and wrote the first draft. All authors contributed to the manuscript. W.-J.S. obtained funding.

Declaration of Competing Interest

The authors declare no conflict of interest.

Acknowledgements

This work was supported by Japan MEXT grants (#15H01442, #17H05749 and #H19H05222) and a JSPS grant (#19K06908).

References

Aramakis, V., Hsieh, C., Leslie, F., Metherate, R., 2000. A critical period for nicotine-induced disruption of synaptic development in rat auditory cortex. J. Neurosci. 20, 6106–6116.
Babola, T.A., Li, S., Gribizis, A., Lee, B.J., Issa, J.B., Wang, H.C., Crair, M.C., Bergles, D.E., 2018. Homeostatic control of spontaneous activity in the developing auditory system. Neuron 99 (3), 511–524.
Baloch, S., Verma, R., Huang, H., Khurd, P., Clark, S., Yarowsky, P., Abel, T., Mori, S., Davatzikos, C., 2009. Quantification of brain maturation and growth patterns in C57BL/6J mice via computational neuroanatomy of diffusion tensor images. Cereb. Cortex 19, 675–687.
Bao, S., Chan, V.T., Merzenich, M.M., 2001. Cortical remodelling induced by activity of ventral tegmental dopamine neurons. Nature 412 (6842), 79–83.
Barkat, T.R., Polley, D.B., Hensch, T.K., 2011. A critical period for auditory thalamocortical connectivity. Nat. Neurosci. 14 (9), 1189–1194.
Blundon, J.A., Roy, N.C., Teubner, B.J.W., Yu, J., Eom, T.-Y., Sample, K.J., Pani, A., Smeyne, R.J., Han, S.B., Kerekes, R.A., Rose, D.C., Hackett, T.A., Vuppala, P.K., Freeman, B.B., Zakharenko, S.S., 2017. Restoring auditory cortex plasticity in adult mice by restricting thalamic adenosine signaling. Science 356 (6345), 1352–1356.
Budinger, E., Heil, P., Scheich, H., 2000. Functional organization of auditory cortex in the Mongolian gerbil (Meriones unguiculatus). III. Anatomical subdivisions and corticocortical connections. Eur. J. Neurosci. 12, 2425–2451.
Cadwell, C.R., Bhaduri, A., Mostajo-Radji, M.A., Keefe, M.G., Nowakowski, T.J., 2019. Development and arealization of the cerebral cortex. Neuron 103 (6), 980–1004.
Chang, E.F., Merzenich, M.M., 2003. Environmental noise retards auditory cortical development. Science 300 (5618), 498–502.
Chen, W., Helmchen, F., Lütcke, H., 2015. Specific early and late oddball-evoked responses in excitatory and inhibitory neurons of mouse auditory cortex. J. Neurosci. 35 (36), 12560–12573.
Chuang, N., Mori, S., Yamamoto, A., Jiang, H., Ye, X., Xu, X., Richards, L.J., Nathans, J., Miller, M.I., Toga, A.W., Sidman, R.L., Zhang, J., 2011. An MRI-based atlas and database of the developing mouse brain. Neuroimage 54, 80–89.
Clause, A., Kim, G., Sonntag, M., Weisz, C.J.C., Vetter, D.E., Rübsamen, R., Karl Kandler, K., 2014. The precise temporal pattern of pre-hearing spontaneous activity is necessary for tonotopic map refinement. Neuron 82 (4), 822–835.
de Villers-Sidani, E., Chang, E.F., Bao, S., Merzenich, M.M., 2007. Critical period window for spectral tuning defined in the primary auditory cortex (A1) in the rat. J. Neurosci. 27 (1), 180–189.
Erzurumlu, R.S., Gaspar, P., 2012. Development and critical period plasticity of the barrel cortex. Eur. J. Neurosci. 35 (10), 1540–1553.
Espinosa, J.S., Stryker, M.P., 2012. Development and plasticity of the primary visual cortex. Neuron 75 (2), 230–249.
Fox, K., 2009. Experience-dependent plasticity mechanisms for neural rehabilitation in somatosensory cortex. Philos. Trans. R. Soc. Lond. B Biol. Sci. 364 (1515), 369–381.
Froemke, R.C., Jones, B.J., 2011. Development of auditory cortical synaptic receptive fields. Neurosci. Biobehav. Rev. 35 (10), 2105–2113.
Geal-Dor, M., Freeman, S., Li, G., Sohmer, H., 1993. Development of hearing in neonatal rats: air and bone conducted ABR thresholds. Hear. Res. 69 (1–2), 236–242.
Grinvald, A., Lieke, E.E., Frostig, R.D., Hildesheim, R., 1994. Cortical point-spread function and long-range lateral interactions revealed by real-time optical imaging of macaque monkey primary visual cortex. J. Neurosci. 14, 2545–2568.
Guo, W., Chambers, A.R., Darrow, K.N., Hancock, K.E., Shinn-Cunningham, B.G., Polley, D.B., 2012. Robustness of cortical topography across fields, laminae, anesthetic states, and neurophysiological signal types. J. Neurosci. 32, 9159–9172.
Hackett, T.A., Barkat, T.R., O'Brien, B.M.J., Hensch, T.K., Polley, D.B., 2011. Linking topography to tonotopy in the mouse auditory thalamocortical circuit. J. Neurosci. 31, 2983–2995.
Hensch, T.K., 2005. Critical period plasticity in local cortical circuits. Nat. Rev. Neurosci. 6 (11), 877–888.
Horie, M., Tsukano, H., Hishida, R., Takebayashi, H., Shibuki, K., 2013. Dual compartments of the ventral division of the medial geniculate body projecting to the core region of the auditory cortex in C57BL/6 mice. Neurosci. Res. 76, 207–212.
Horikawa, J., Hess, A., Nasu, M., Hosokawa, Y., Scheich, H., Taniguchi, I., 2001. Optical imaging of neural activity in multiple auditory cortical fields of guinea pigs. Neuroreport 12, 3335–3339.
Horikawa, J., Hosokawa, Y., Kubota, M., Nasu, M., Taniguchi, I., 1996. Optical imaging of spatiotemporal patterns of glutamatergic excitation and GABAergic inhibition in the guinea-pig auditory cortex in vivo. J. Physiol. 497, 629–638.
Imaizumi, K., Priebe, N.J., Crum, P.A., Bedenbaugh, P.H., Cheung, S.W., Schreiner, C.E., 2004. Modular functional organization of cat anterior auditory field. J. Neurophysiol. 92, 444–457.
Imaizumi, K., Schreiner, C.E., 2007. Spatial interaction between spectral integration and frequency gradient in primary auditory cortex. J. Neurophysiol. 98, 2933–2942.
Inan, M., Crair, M.C., 2007. Development of cortical maps: perspectives from the barrel cortex. Neuroscientist 13 (1), 49–61.
Issa, J.B., Haeffele, B.D., Agarwal, A., Bergles, D.E., Young, E.D., Yue, D.T., 2014. Multiscale optical Ca^{2+} imaging of tonal organization in mouse auditory cortex. Neuron 83 (4), 944–959.
Jacobson, S., 1963. Sequence of myelinization in the brain of the albino rat. a. cerebral cortex, thalamus and related structures. J. Comp. Neurol. 121, 5–29.
Kaas, J.H., Hackett, T.A., 2000. Subdivisions of auditory cortex and processing streams in primates. Proc. Natl. Acad. Sci. USA 97, 11793–11799.
Kalatsky, V.A., Polley, D.B., Merzenich, M.M., Schreiner, C.E., Stryker, M.P., 2005. Fine functional organization of auditory cortex revealed by Fourier optical imaging. Proc. Natl. Acad. Sci. USA 102, 13325–13330.
Keuroghlian, A.S., Knudsen, E.I., 2007. Adaptive auditory plasticity in developing and adult animals. Prog. Neurobiol. 82 (3), 109–121.
Kobayashi, T., 1963. Brain-to-body ratios and time of maturation of the mouse brain. Am. J. Physiol. 204, 343–346.
Kral, A., Pallas, S.L., 2011. Development of the auditory cortex. In: The Auditory Cortex. Springer, pp. 443–463.
Kubota, Y., Kamatani, D., Tsukano, H., Ohshima, S., Takahashi, K., Hishida, R., Kudoh, M., Takahashi, S., Shibuki, K., 2008. Transcranial photo-inactivation of neural activities in the mouse auditory cortex. Neurosci. Res. 60 (4), 422–430.
Liberman, M.C., 1982. The cochlear frequency map for the cat: labeling auditory-nerve fibers of known characteristic frequency. J. Acoust. Soc. Am. 72, 1441–1449.
Linden, J.F., Liu, R.C., Sahani, M., Schreiner, C.E., Merzenich, M.M., 2003. Spectrotemporal structure of receptive fields in areas AI and AAF of mouse auditory cortex. J. Neurophysiol. 90, 2660–2675.
Meredith, M.A., Lomber, S.G., 2011. Somatosensory and visual crossmodal plasticity in the anterior auditory field of early-deaf cats. Hear. Res. 280 (1–2), 38–47.
Mrsic-Flogel, T.D., Schnupp, J.W.H., King, A.J., 2003. Acoustic factors govern developmental sharpening of spatial tuning in the auditory cortex. Nat. Neurosci. 6, 981–988.
Mrsic-Flogel, T.D., Versnel, H., King, A.J., 2006. Development of contralateral and ipsilateral frequency representations in ferret primary auditory cortex. Eur. J. Neurosci. 23, 780–792.
Nakata, S., Takemoto, M., Song, W.-J., 2020. Differential cortical and subcortical projection targets of subfields in the core region of mouse auditory cortex. Hear. Res. 386, 107876.
Nishimura, M., Shirasawa, H., Kaizo, H., Song, W.-J., 2007. New field with tonotopic organization in guinea pig auditory cortex. J. Neurophysiol. 97, 927–932.
Nishimura, M., Song, W.-J., 2014. Greenwood frequency-position relationship in the primary auditory cortex in guinea pigs. NeuroImage 89, 181–191.
Nishimura, M., Takemoto, M., Song, W.-J., 2018. Organization of auditory areas in the superior temporal gyrus of marmoset monkeys revealed by real-time optical imaging. Brain Struct. Funct. 223 (4), 1599–1614.
Oswald, A.M.M., Reyes, A.D., 2011. Development of inhibitory timescales in auditory cortex. Cereb. Cortex 21 (6), 1351–1361.
Pickles, J.O., 2008. An Introduction to the Physiology of Hearing, third ed. Emerald.
Polley, D.B., Read, H.L., Storace, D.A., Merzenich, M.M., 2007. Multiparametric auditory receptive field organization across five cortical fields in the albino rat. J. Neurophysiol. 97, 3621–3638.

Polley, D.B., Thompson, J.H., Guo, W., 2013. Brief hearing loss disrupts binaural integration during two early critical periods of auditory cortex development. Nat. Commun. 4, 2547.
Ray, S., Brecht, M., 2016. Structural development and dorsoventral maturation of the medial entorhinal cortex. Elife 5, e13343.
Reinhard, S.M., Abundez-Toledo, M., Espinoza, K., Razak, K.A., 2019. Effects of developmental noise exposure on inhibitory cell densities and perineuronal nets in A1 and AAF of mice. Hear. Res. 381, 107781.
Romero, S., Hight, A.E., Clayton, K.K., Resnik, J., Williamson, R.S., Hancock, K.E., Polley, D.B., 2020. Cellular and widefield imaging of sound frequency organization in primary and higher-order fields of the mouse auditory cortex. Cereb. Cortex 30 (3), 1603–1622.
Sakano, H., 2020. Developmental regulation of olfactory circuit formation in mice. Dev. Growth Differ. 62, 199–213.
Saldeitis, K., Happel, M.F., Ohl, F.W., Scheich, H., Budinger, E., 2014. Anatomy of the auditory thalamocortical system in the Mongolian gerbil: nuclear origins and cortical field-, layer-, and frequency-specificities. J. Comp. Neurol. 522, 2397–2430.
Sanes, D.H., Bao, S., 2009. Tuning up the developing auditory CNS. Curr. Opin. Neurobiol. 19 (2), 188–199.
Sawatari, H., Tanaka, Y., Takemoto, M., Nishimura, M., Hasegawa, K., Saitoh, K., Song, W.-J., 2011. Identification and characterization of an insular auditory field in mice. Eur. J. Neurosci. 34, 1944–1952.
Semple, B.D., Blomgren, K., Gimlin, K., Ferriero, D.M., Noble-Haeusslein, L.J., 2013. Brain development in rodents and humans: Identifying benchmarks of maturation and vulnerability to injury across species. Prog. Neurobiol. 0, 1–16.
Shatz, C.J., 1997. Form from function in visual system development. Harvey Lect. 93, 17–34.
Shepard, K.N., Liles, L.C., Weinshenker, D., Liu, R.C., 2015. Norepinephrine is necessary for experience-dependent plasticity in the developing mouse auditory cortex. J. Neurosci. 35 (6), 2432–2437.
Shoham, D., Glaser, D.E., Arieli, A., Kenet, T., Wijnbergen, C., Toledo, Y., Hildesheim, R., Grinvald, A., 1999. Imaging cortical dynamics at high spatial and temporal resolution with novel blue voltage-sensitive dyes. Neuron 24, 791–802.
Schreiner, C.E., Urbas, J.V., 1988. Representation of amplitude modulation in the auditory cortex of the cat. II. Comparison between cortical fields. Hear. Res. 32, 49–63.
Sollini, J., Chapuis, G.A., Clopath, C., Chadderton, P., 2018. ON-OFF receptive fields in auditory cortex diverge during development and contribute to directional sweep selectivity. Nat. Commun. 9 (1), 2084.
Song, W.-J., Kawaguchi, H., Totoki, S., Inoue, Y., Katura, T., Maeda, S., Inagaki, S., Shirasawa, H., Nishimura, M., 2006. Cortical intrinsic circuits can support activity propagation through an isofrequency strip of the guinea pig primary auditory cortex. Cereb. Cortex 16, 718–729.
Sołyga, M., Barkat, T.R., 2019. Distinct processing of tone offset in two primary auditory cortices. Sci. Rep. 9 Article number: 9581.
Stiebler, I., Neulist, R., Fichtel, I., Ehret, G., 1997. The auditory cortex of the house mouse: left-right differences, tonotopic organization and quantitative analysis of frequency representation. J. Comp. Physiol. A 181, 559–571.
Storace, D.A., Higgins, N.C., Read, H.L., 2011. Thalamocortical pathway specialization for sound frequency resolution. J. Comp. Neurol. 519, 177–193.
Takahashi, K., Hishida, R., Kubota, Y., Kudoh, M., Takahashi, S., Shibuki, K., 2006. Transcranial fluorescence imaging of auditory cortical plasticity regulated by acoustic environments in mice. Eur. J. Neurosci. 23 (5), 1365–1376.
Takemoto, M., Hasegawa, K., Nishimura, M., Song, W.-J., 2014. The insular auditory field receives input from the lemniscal subdivision of the auditory thalamus in mice. J. Comp. Neurol. 522, 1373–1389.
Tokioka, R., Kawaguchi, H., Fukunishi, K., 2000. Spatio-temporal analyses of stimulus-evoked and spontaneous stochastic neural activity observed by optical imaging in guinea pig auditory cortex. Brain Res. 861, 271–280.
Tsukano, H., Horie, M., Ohga, S., Takahashi, K., Kubota, Y., Hishida, R., Takebayashi, H., Shibuki, K., 2017. Reconsidering Tonotopic maps in the auditory cortex and lemniscal auditory thalamus in mice. Front. Neural Circt. 11, 14.
Tsukano, H., Horie, M., Bo, T., Uchimura, A., Hishida, R., Kudoh, M., Takahashi, K., Takebayashi, H., Shibuki, K., 2015. Delineation of a frequency-organized region isolated from the mouse primary auditory cortex. J. Neurophysiol. 113 (7), 2900–2920.
Wallace, M.N., Rutkowski, R.G., Palmer, A.R., 2000. Identification and localisation of auditory areas in guinea pig cortex. Exp. Brain Res. 132, 445–456.
Wang, H.C., Bergles, D.E., 2015. Spontaneous activity in the developing auditory system. Cell Tissue Res. 361, 65–75.
Watson, R.E., Desesso, J.M., Hurtt, M.E., Cappon, G.D., 2006. Postnatal growth and morphological development of the brain: a species comparison. Birth Defects Res. B Dev. Reprod. Toxicol. 77 (5), 471–484.
Zhang, L.I., Bao, S., Merzenich, M.M., 2001. Persistent and specific influences of early acoustic environments on primary auditory cortex. Nat. Neurosci. 4 (11), 1123–1130.
Yamamoto, N., 2002. Cellular and molecular basis of axonal targeting in the formation of lamina-specific thalamocortical projections. Neurosci. Res. 42, 167–173.